# Technetium-99m-Tetrofosmin for Parathyroid Scintigraphy: Comparison to Thallium–Technetium Scanning

Dimitris J. Apostolopoulos, Evangelia Houstoulaki, Costas Giannakenas, Theodore Alexandrides, John Spiliotis, George Nikiforidis, John G. Vlachojannis and Pavlos J. Vassilakos

*University of Patras Medical School, Patras; and Departments of Nuclear Medicine, Endocrinology, Surgery, Medical Physics and Nephrology, Regional University Hospital of Patras, Patras, Greece*

The efficacy of $^{99m}$Tc-tetrofosmin for the detection of parathyroid lesions was investigated prospectively in patients with hyperparathyroidism referred for surgical treatment. **Methods:** Twenty-seven patients with primary and 18 with tertiary hyperparathyroidism were studied. Twelve patients had undergone one or more previous neck explorations. Static imaging with $^{201}$Tl was performed first, immediately followed by a 30-min $^{99m}$Tc-tetrofosmin dynamic study. Delayed views of up to 3 hr postinjection were also obtained. Technetium-99m-pertechnetate was used for thyroid delineation. The tetrofosmin/$^{99m}$Tc-pertechnetate subtraction scan (TF/TC), the single-tracer washout technique and the thallium/technetium subtraction (TL/TC) were compared. Quantification of relative uptakes of tracers in the thyroid and abnormal parathyroids was accomplished by measuring activity within regions of interest. Kinetics of tetrofosmin in the thyroid and abnormal parathyroids were studied by evaluating the plots of the parathyroid to thyroid ratios against time as well as by calculation of the half-clearance times from the slow component of the time-activity curves. **Results:** The overall sensitivity, specificity and accuracy of TF/TC and TL/TC were 76%, 92% and 83% and 52%, 85% and 65%, respectively. The respective sensitivities were 87% and 70% for adenomas and 72% and 46% for hyperplasia. The parathyroid-to-thyroid activity ratios of tetrofosmin were significantly higher than those of thallium ($p < 0.001$). The tetrofosmin single-tracer washout study was less accurate than the subtraction technique (overall sensitivity and specificity, 70% and 69%, respectively). The washout properties of tetrofosmin in abnormal parathyroids were not substantially different from those in the thyroid, with a few exceptions ($p = 0.4$). No correlation of half-clearance times with parathyroid size, degree of early uptake, parathyroid hormone levels or histology could be established. Comparing adenomas to hyperplasia in respect to tetrofosmin retention, a statistically significant difference was observed ($p = 0.005$). **Conclusion:** Technetium-99m-tetrofosmin is suitable for parathyroid imaging. The kinetic properties of this agent in parathyroid and thyroid tissues do not warrant differential washout protocols. The diagnostic impact of the observed difference in tetrofosmin kinetics between parathyroid adenomas and hyperplasia requires further investigation.

**Key Words:** parathyroid scintigraphy; technetium-99m-tetrofosmin; thallium–technetium subtraction scan; comparison

**J Nucl Med 1998; 39:1433–1441**

Since the initial description of the technique by Ferlin et al. (*1*), thallium–technetium (TL/TC) subtraction scanning has been implemented for over a decade for the localization of abnormal parathyroid glands. The reported sensitivity of the method is highly variable but usually lies within the range of 70–90% for parathyroid adenomas (*2–7*), whereas regarding hyperplasia figures are considerably lower (*8–10*). Technetium-99m-sestamibi has been proposed as a substitute for thallium; superior image quality, more favorable dosimetry, $^{99m}$Tc availability and higher sensitivity postulate are its advantages (*11–15*). The differential washout properties of $^{99m}$Tc-sestamibi in thyroid and parathyroid tissues have enabled double-phase and washout kinetic studies (*16,17*), which have been reported to obviate the need of a second tracer and problems induced by subtraction. Technetium-99m-tetrofosmin has been recently introduced as a myocardial perfusion agent (*18*). Similarities in biodistribution and biokinetics between these two technetium agents (*19,20*) have triggered research toward the same fields of application. To date, only a few reports pertaining to the use of $^{99m}$Tc-tetrofosmin for parathyroid imaging have appeared in the literature (*21–24*).

The aim of this work was to assess $^{99m}$Tc-tetrofosmin as a parathyroid-localizing agent. The results are compared to those of the conventional TL/TC subtraction scan. Kinetic properties of this new agent in the thyroid and in abnormal parathyroids are also addressed to define the optimal imaging times and technique.

## MATERIALS AND METHODS

Over a period of 10 mo 59 consecutive patients referred to our laboratory for a TL/TC scan were also studied with $^{99m}$Tc-tetrofosmin. All patients as well as the referring physicians had been previously informed of the purpose and the procedure of the study and had given their consent. Forty-five patients (31 women, 14 men; age range 22–78 yr; mean age 57.8 yr) subsequently underwent explorative neck surgery. Twelve of these had already experienced one or more previous neck explorations. In 27 of the patients, the diagnosis of primary hyperparathyroidism had been established on biochemical grounds, whereas another 18 patients suffered from end-stage renal failure and had evidence of tertiary hyperparathyroidism. Preoperative parathyroid hormone (PTH) levels were determined by an immunoradiometric assay that measures the intact molecule (ELSA-PTH; Cis Bio-International, Maccoule, France). Values averaged from repeated measurements ranged from 80–367 pg/ml (mean = 142 pg/ml; median = 149 pg/ml) in the primary hyperparathyroidism group (normal range 10–70 pg/ml); in the patients with renal failure, PTH levels determined from undiluted serum samples ranged from 276 pg/ml to over 1500 pg/ml (median = 975 pg/ml).

Ninety-one enlarged parathyroids were identified during surgery. Most of them were removed, the others were half-excised (in cases of four gland hyperplasia), and the remnants were either clipped or autotransplanted. The weight of the removed parathyroids ranged from 105 mg to 3.8 g. Gross surgical findings

Received Jan. 9, 1997; revision accepted Nov. 21, 1997.

For correspondence or reprints contact: Dimitris J. Apostolopoulos, MD, Department of Nuclear Medicine, University of Patras Medical School, Regional University Hospital of Patras, Rion Patras 26500, Greece.

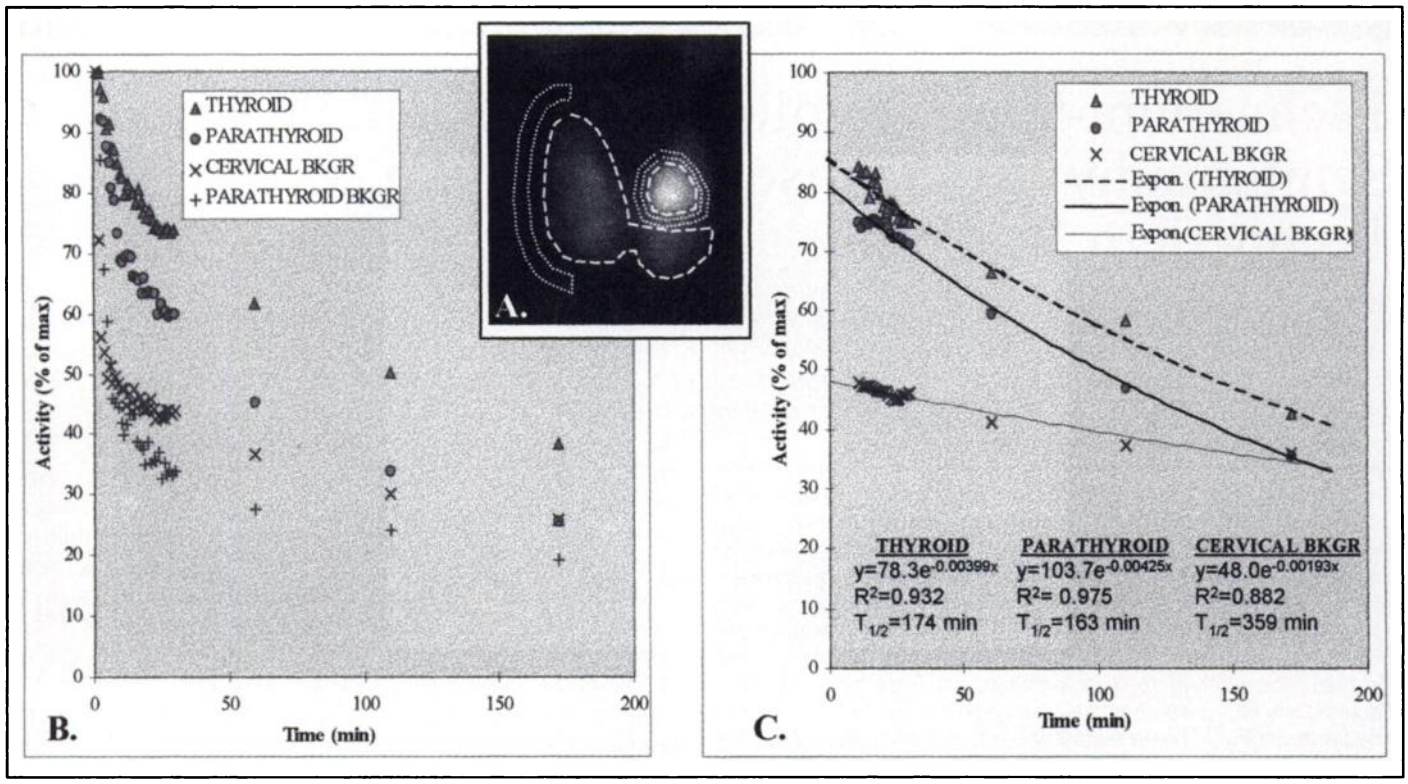


**FIGURE 1.** (A) Tetrofosmin image with ROIs, in a case of a left upper parathyroid adenoma. (B) Corresponding time-activity curves from original data, before background and $^{99m}$Tc decay correction. (C) First-order exponential function fitted in corrected data beyond the 10th min. The equation formula, the $R^2$ value of regression and the calculated half-clearance time are shown.

combined with histologic examination reported 23 solitary parathyroid adenomas, 8 hyperplastic parathyroids in 4 patients with primary hyperparathyroidism and 60 hyperplastic glands in the group of patients with renal failure. In 1 patient, a medullary thyroid carcinoma was incidentally found during surgery. No other patients had evidence that their hyperparathyroidism was part of a multiple endocrine neoplasm syndrome. All patients were biochemically cured in the short postsurgical follow-up period (1–9 mo).

### Acquisition

The scintigraphic acquisition and processing was performed with a dual-head gamma camera system (Helix, Elscint, Israel) using a pinhole collimator on one head and an all-purpose parallel-hole collimator on the other. The pinhole collimator placed 8 cm above the patient's neck, along with a zoom factor of 3, on a 128 × 128 matrix was used for obtaining high resolution images of the neck. The parallel-hole collimator provided a wider field for viewing the entire mediastinum; the settings in this instance were 256 × 256, zoom 1. Switching from one collimator to the other required only the few seconds needed to rotate the gantry by 180°. Thallium-201 chloride (CIS Bio-International) was injected first in a dose of 74–92 MBq. An anterior image of the mediastinum was acquired 10 min later, followed by an image of the neck. A total of 600 and 200 kilocounts, respectively, were obtained. Technetium-99m-tetrofosmin was reconstituted from a cold lyophilized kit (Myoview; Amersham, Aylesbury, United Kingdom) according to the manufacturer's instructions. One to three doses were drawn from each vial. Labeling efficiency assessed by thin-layer chromatography was greater than 95% in all cases. Three-hundred seventy MBq was administered immediately after the completion of thallium acquisition. A dynamic series of images (one frame per minute) was acquired for the next 30 min. A view of the mediastinum was subsequently obtained. Three or four delayed images, between 1 and 3 hr postinjection, were also acquired in all patients. The thyroid scans were performed on the same day with $^{99m}$Tc-pertechnetate, unless a low uptake of pertechnetate was suspected from the patient's history. Twenty minutes after the injection of 300–370 MBq $^{99m}$Tc-pertechnetate (150 MBq in cases where imaging was performed on a separate day) 300 kilocounts were obtained. Radioactive markers were used to aid correct repositioning of the patient at the different phases of the study.

### Processing

The dynamically acquired set of tetrofosmin images was replayed in cinematic display mode, and motion correction was applied if necessary. Three images generated from the reframed dynamic series were reproduced on hardcopy, together with the delayed images. The manufacturer's computer software, slightly modified, was used for thallium–pertechnetate and TF/TC subtraction. A cumulative image of tetrofosmin generated from the summation of the 11th to the 20th frames of the dynamic series was selected for the subtraction procedure. Separate hardcopies of the TL/TC and TF/TC subtraction studies were reproduced.

Manual ROIs were drawn over the areas of normal thyroid tissue (excluding all focal abnormalities) and of the suspected sites of parathyroid lesions, as indicated by the results of subtraction. Cervical background activity was represented by a crescent-shaped region of interest (ROI) lateral to the thyroid. For background correction of parathyroid activity, circular ROIs (two pixels wide and two pixels apart from the reference ROI) were drawn automatically around the suspected parathyroid regions (Fig. 1A).

Parathyroid-to-thyroid activity ratios (PAR/THYR), normalized for the ROI area, and thyroid-to-cervical background ratios (THYR/BKGR) were calculated from thallium and tetrofosmin images. The parathyroid-to-background ratio (PAR/BKGR) was computed whenever the parathyroid lesions were visualized outside the thyroid borders, either totally or in their greater part. In the remaining cases this estimation was omitted, as it only duplicated the PAR/THYR ratio (the thyroid itself was the actual background

**TABLE 1**
True-Positive Findings of TL/TC and TF/TC Subtraction Scintigraphy

| Histology | Surgery (+) (n) | TL/TC (+) (n (sens)) | TF/TC (+) (n (sens)) | Difference: TF/TC (+) TL/TC (−) (n) | Difference: TF/TC (−) TL/TC (+) (n) | Statistics, McNemar test (p) |
|---|---|---|---|---|---|---|
| Adenoma | 23 | 16 (70) | 20 (87) | 4 | 0 | 0.13 |
| Hyperplasia | 68 | 31 (46) | 49 (72) | 19 | 1 | 0.00006 |
| Total | 91 | 47 (52) | 69 (76) | 23 | 1 | 0.00001 |

The difference between the two methods is statistically evaluated. sens = sensitivity. Percentages are given in parentheses.

to the parathyroid in these circumstances). Ratios integrated from the 11th to the 20th min of tetrofosmin dynamic acquisition were compared with those of thallium. Only data from true-positive findings were evaluated.

### Interpretation

The randomized hard copies of the scintigraphic studies were independently reviewed by two experienced nuclear physicians. Apart from the TL/TC and the TF/TC subtraction, a set of six or seven serial tetrofosmin images was interpreted as a single-tracer washout study in each patient. Reviewers were blind to the surgical findings and to all other information (patient's history, findings of other localization methods and so on). A distinct focus of activity of thallium or tetrofosmin, not attributable to functional thyroid tissue, was the criterion of a positive finding for the subtraction studies. As for the single tracer studies of tetrofosmin, a focus exceeding thyroid activity as well as all extrathyroidal foci (except the salivary glands), in either the early or the delayed images, was the criterion of positivity. The time that the lesions were more prominent (early or late images) was reported in each case. Scintigraphic findings were classified as positive for parathyroid enlargement in a certain location if both interpreters had independently reached the same conclusion. Ambiguous findings, as well as discordant results between the two observers were scored negative. Finally, the scintigraphic results were compared to the surgical findings.

### Kinetics of Technetium-99m-Tetrofosmin

Activity normalized for the ROI area over the thyroid, the parathyroids and the corresponding background regions was plotted against time (Fig. 1B). An exponential function was used to fit data points beyond the first 10 min of acquisition, after correction for background and $^{99m}$Tc decay. Fitting was considered satisfactory if the $R^2$ value of regression was greater than 0.7; otherwise, results were excluded. Half-clearance times ($T_{1/2}$) of tetrofosmin from the surgically confirmed parathyroid abnormalities, the thyroid and the cervical background regions were calculated (Fig. 1C). All previously mentioned ratios (THYR/BKGR, PAR/THYR and PAR/BKGR) were also plotted against time in separate charts.

## RESULTS

### Qualitative Comparison Results

Forty-seven enlarged parathyroid glands were identified and correctly localized by the TL/TC scan. Four of these were ectopic; 1 below the right salivary gland and 3 in the mediastinum (2 subclavicularly, accessible through a neck incision, and 1 lower, accessible via medial sternotomy). The smallest parathyroid gland detected (among those totally removed) weighed 390 mg. The largest missed parathyroid weighed 1.2 g. Of the missed lesions, all but 1 were orthotopic. Seven of 10 false-positive sites of thallium were attributed to nonfunctioning thyroid nodules, whereas artifacts of the subtraction procedure were the most probable cause of the other three.

On the other hand, the TF/TC scan correctly localized 69 abnormal parathyroids, 62 in the neck, 3 in the subclavicular area and 1 lower in the mediastinum, whereas it missed 22 glands, all orthotopic. The smallest gland identified by tetrofosmin and the largest missed weighed 180 and 750 mg, respectively. Five false-positive findings were all attributed to nonfunctioning thyroid nodules.

Comparing the two subtraction methods, the TF/TC scan led to the detection of more parathyroid adenomas and more hyperplastic glands, while producing fewer false-positive findings (Tables 1 and 2). Regarding sensitivity, statistical significance was reached in the parathyroid hyperplasia group, but not in parathyroid adenomas (Table 1). In one case, the TL/TC scan revealed a hyperplastic parathyroid gland while the TF/TC scan was negative; an adenoma of the thyroid overlying the enlarged parathyroid was found intraoperatively. It was not clear whether thallium depicted the thyroid or the parathyroid adenoma in this case. With this exception, there were no true-positive findings on the TL/TC studies that were not also evident in the TF/TC scan. In one patient in whom a medullary thyroid carcinoma as well as two hyperplastic parathyroid glands were found intraoperatively, none of these abnormalities had been preoperatively depicted by either method.

Interpretation of tetrofosmin serial images as a single-tracer study compared to the TF/TC subtraction missed five other parathyroid lesions; the false-positives increased to 20, mainly due to misinterpretation of autonomously functioning thyroid nodules. Both interpreters agreed that delayed images were helpful in 3 cases of parathyroid adenoma and 1 case of hyperplasia, providing better distinction of the lesion from the overlying thyroid than the early images. However, in all 4 of these cases the subtraction technique had succeeded in disclosing the parathyroid abnormality. The overall performance of the tetrofosmin single-tracer and the two subtraction techniques are shown in Table 2. The total of 65 surgically identified normal parathyroids was taken as a reference of the negative sites.

Preoperative studies of TL/TC and TF/TC subtraction scans in two cases of solitary parathyroid adenomas and one of parathyroid hyperplasia are shown in Figures 2–4. The higher uptake of tetrofosmin by parathyroid lesions relative to the

**TABLE 2**
Diagnostic Evaluation of TL/TC, TF/TC Subtraction Techniques and Tetrofosmin Single-Tracer Scintigraphy

| | Sensitivity | Specificity | False-positive rate | Accuracy |
|---|---|---|---|---|
| TL/TC | 47/91 (52) | 55/65 (85) | 10/65 (15) | 102/156 (65) |
| TF/TC | 69/91 (76) | 60/65 (92) | 5/65 (8) | 129/156 (83) |
| TF single-tracer | 64/91 (70) | 45/65 (69) | 20/65 (31) | 109/156 (70) |

Values are numbers of cases, with the percentage in parentheses.

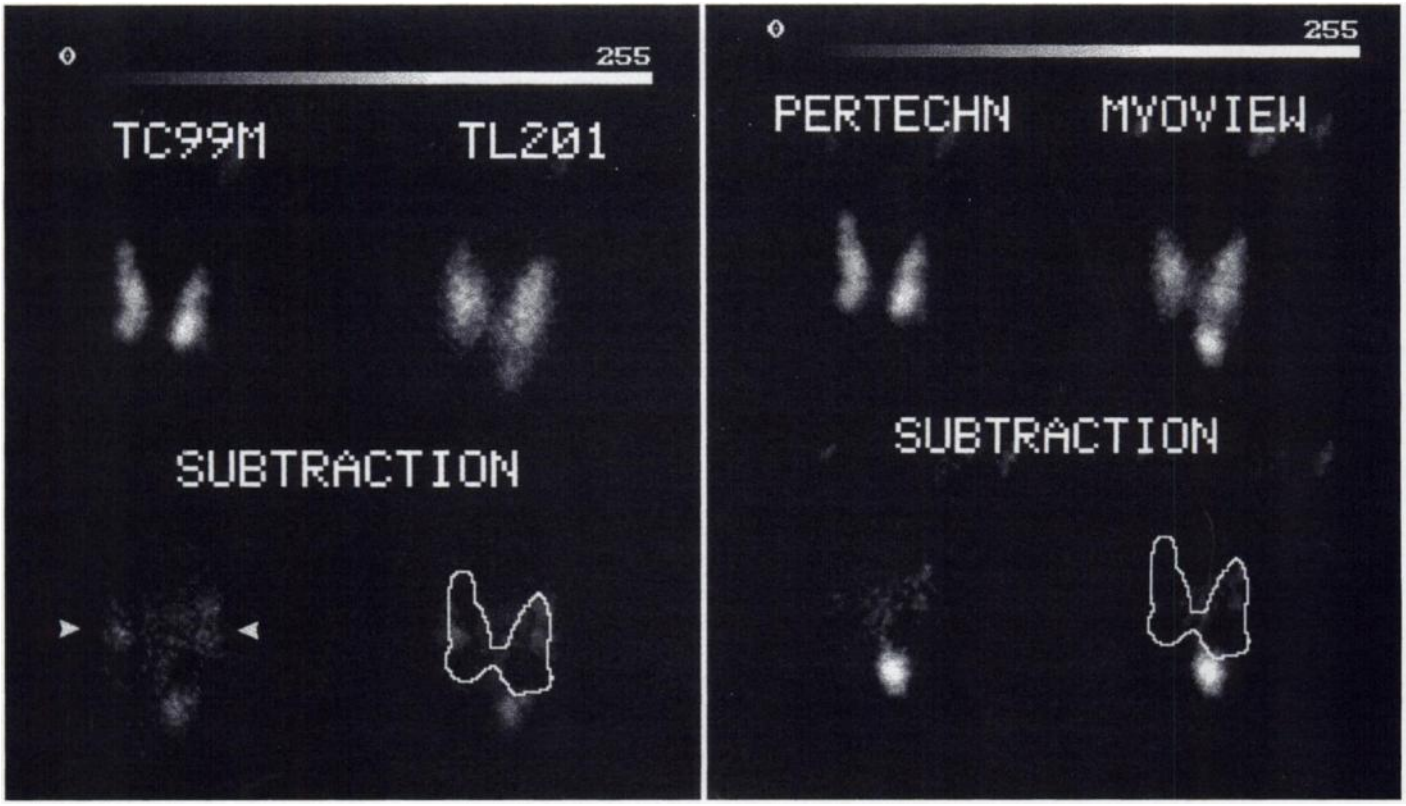


**FIGURE 2.** Subtraction studies of TL/TC (left) and of TF/TC (right). In this case, an adenoma of the left lower parathyroid weighing 1000 mg was correctly localized by both methods. Compared to that of thallium, the higher uptake of tetrofosmin by the adenoma is apparent. False-positive findings due to tracer uptake in the area of nonfunctioning thyroid nodules are more prominent in the thallium subtraction image (arrowheads).

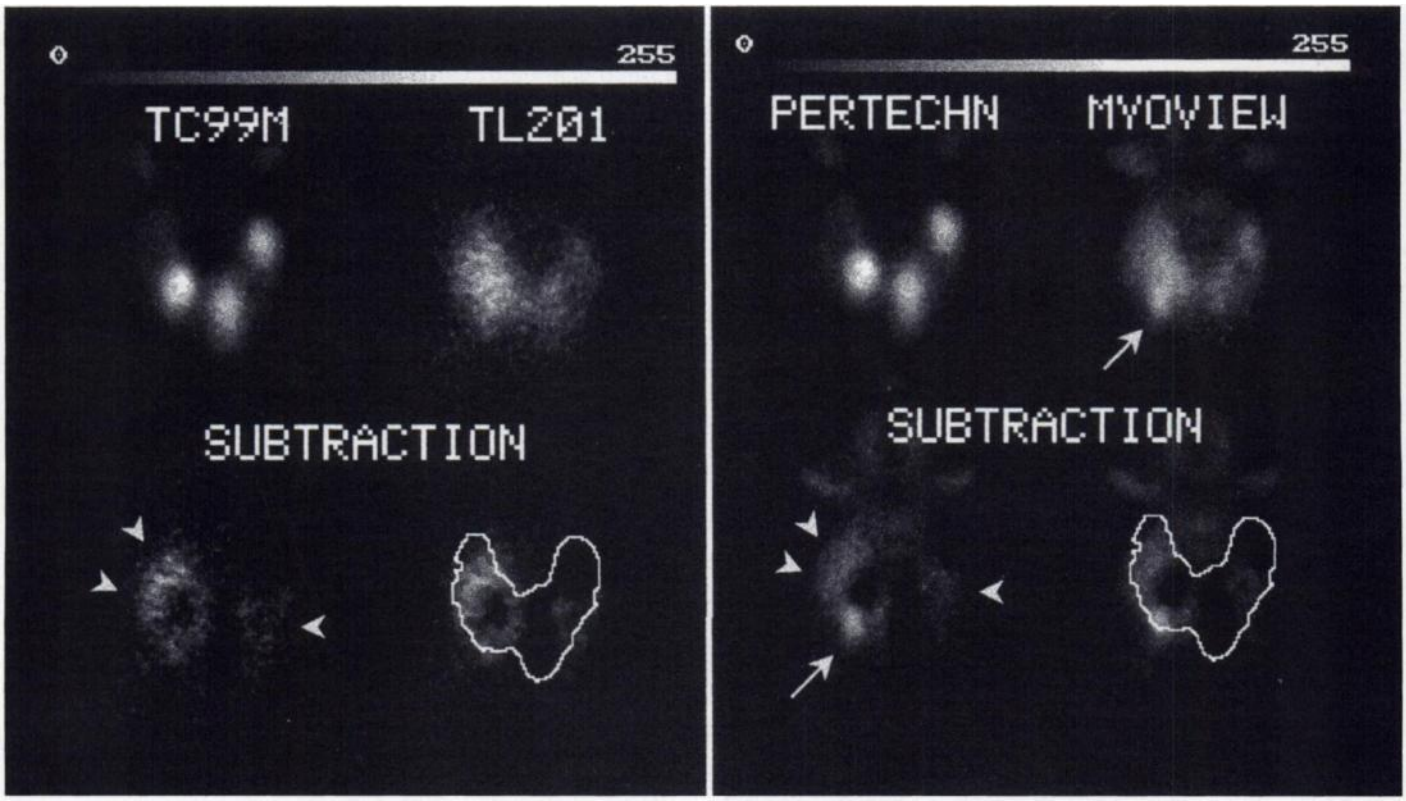


**FIGURE 3.** A solitary parathyroid adenoma weighing 1200 mg, identified only by TF/TC scan (arrow), in a patient with toxic multinodular goiter. Note the areas of the thyroid with suppressed uptake of $^{99m}$Tc-pertechnetate but nonsuppressible uptake of thallium and tetrofosmin and the impact of this discrepancy on the subtracted image (arrowheads). Uptake of tetrofosmin by the parathyroid adenoma exceeds that of the autonomously functioning thyroid adenomas.

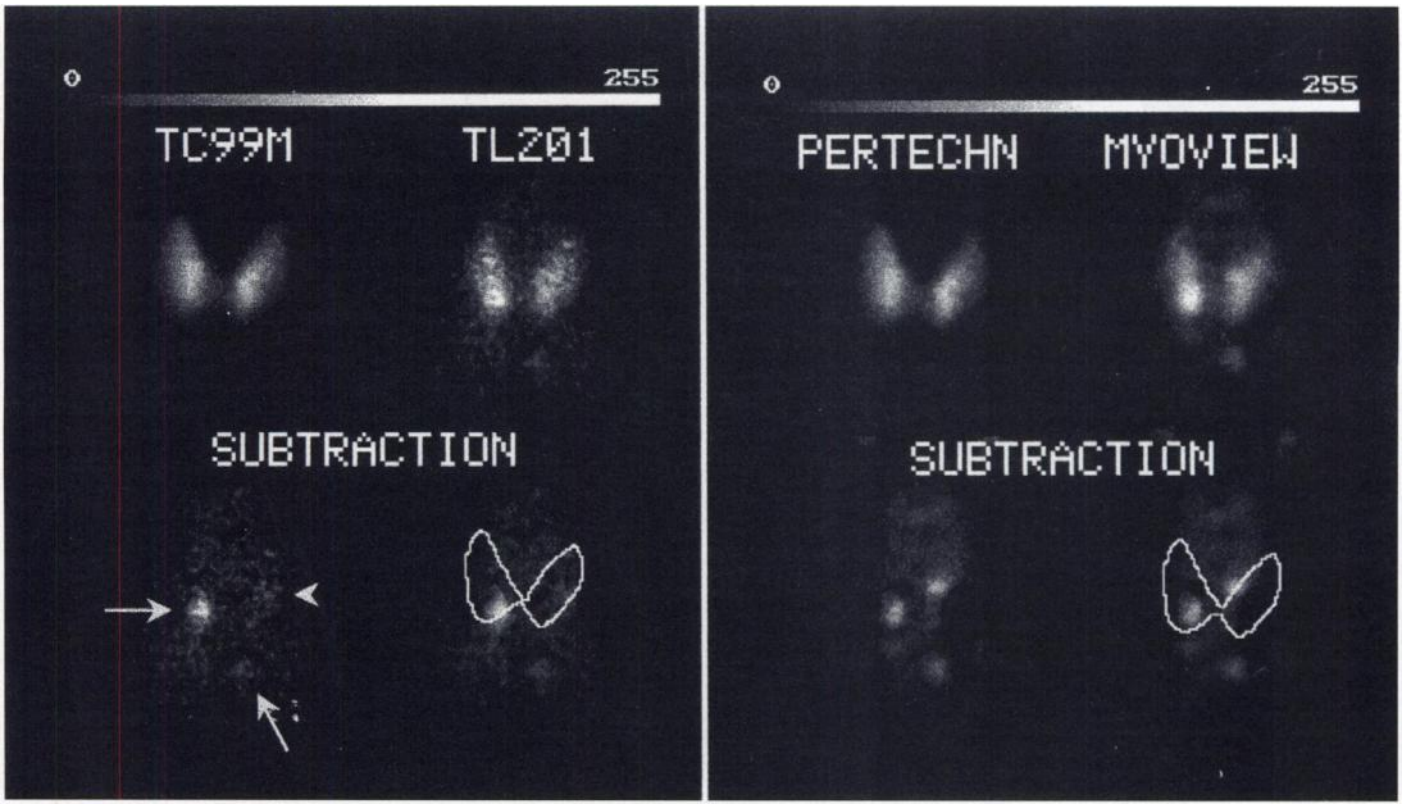


**FIGURE 4.** A case of tertiary hyperparathyroidism is depicted. The TL/TC scan detects two abnormal parathyroids (arrows). A faint focus of thallium activity in the middle of the left thyroidal lobe corresponds to the site of a nonfunctioning thyroid nodule (arrowhead). On the TF/TC scan all four hyperplastic parathyroids are identified, while no false-positive findings are evident in the subtraction image.

thyroid and the detection of more parathyroid abnormalities than with thallium are apparent.

### Quantitative Comparison Results

*THYR/BKGR.* Patients not yet operated on were also included in this evaluation. Calculations were accomplished in 57 of 59 patients (the two other patients had a previous near-total thyroidectomy for papillary carcinoma of the thyroid). The THYR/BKGR ratios of thallium were generally higher than those of tetrofosmin. The difference reached statistical significance only in the group of patients with normal renal function (Table 3).

*PAR/THYR.* Including only data from sites positive to both tracers, the PAR/THYR ratios of tetrofosmin were higher than those of thallium in the vast majority of cases, thus establishing a distinct statistical difference (Table 3).

*PAR/BKGR.* In cases where parathyroids are not visualized within the thyroidal border, the PAR/BKGR rather than the PAR/THYR activity ratio is critical for their scintigraphic detection. Tetrofosmin images usually showed more background activity than thallium images. Despite this, the difference between the two tracers was again significantly in favor of tetrofosmin (Table 3).

### Technetium-99m-Tetrofosmin Kinetics

*Thyroid.* The counts recorded over the region of the thyroid showed an early peak (first or second minute) in all patients. Subsequently, a rapid decrease in activity over the next few minutes was observed, followed by a slower decline over the remaining study time. The time-activity curves resembled a biexponential function (Fig. 1B), in which the early and late

**TABLE 3**
Quantitative Results Comparing the Thallium and Tetrofosmin Relative Uptake Ratios

| Ratio | Pairs (n) | Thallium Mean | Thallium s.d. | Tetrofosmin Mean | Tetrofosmin s.d. | Statistics, Wilcoxon test (p) |
|---|---|---|---|---|---|---|
| THYR/BKGR | | | | | | |
| Normal renal function | 30 | 2.17 | 0.44 | 1.99 | 0.37 | 0.0004 |
| Renal failure | 27 | 1.92 | 0.57 | 1.90 | 0.39 | 0.85 |
| Total | 57 | 2.05 | 0.51 | 1.95 | 0.38 | 0.005 |
| PAR/THYR | | | | | | |
| Within thyroid borders* | 30 | 1.46 | 0.23 | 1.55 | 0.29 | 0.005 |
| Beyond thyroid borders* | 15 | 0.93 | 0.20 | 1.11 | 0.25 | 0.00003 |
| Total | 45 | 1.28 | 0.34 | 1.39 | 0.35 | 0.000002 |
| PAR/BKGR | | | | | | |
| Beyond thyroid borders* | 16 | 1.83 | 0.56 | 1.79 | 0.55 | 0.024 |

*Enlarged parathyroids visualized within or beyong the thyroid borders, completely or in the greater part.
Paired differences from concordant findings of the two agents are statistically evaluated.

**TABLE 4**
Results of the Calculated Half-Clearance Time of Technetium-99m-Tetrofosmin from Abnormal Parathyroid Glands and the Thyroids of the Same Patients

| | Thyroid, tetrofosmin $T_{1/2}$(min) | | | | | Parathyroid, tetrofosmin $T_{1/2}$(min) | | | | | Statistics, Wilcoxon test |
|---|---|---|---|---|---|---|---|---|---|---|---|
| | n | Mean | Median | Range | s.d. | n | Mean | Median | Range | s.d. | (p) |
| Adenoma | 17 | 169 | 142 | 78–317 | 77 | 17 | 240 | 209 | 93–560 | 136 | 0.09 |
| Hyperplasia | 16 | 146 | 137 | 65–311 | 69 | 42 | 149 | 128 | 60–411 | 82 | 0.79 |
| Total | 34 | 158 | 138 | 65–317 | 73 | 59 | 175 | 135 | 60–560 | 108 | 0.41 |

The statistical difference between parathyroid and thyroid is presented.

phases were assumed to represent the vascular and the cellular compartments of the thyroid, respectively. First-order exponential fitting applied to the slow component of the curves yielded evaluable results ($R^2 > 0.7$) in 47 cases. The mean $T_{1/2} \pm$ s.d. was 169 ± 64 min (range = 65–317, median = 160).

*Cervical Background.* The maximum counting rate over the background regions was always observed in the first minute of acquisition. After a very sharp decline over the next few minutes, background activity remained relatively stable, with a mean $T_{1/2}$ of 588 ± 235 min (range = 265–1277, median = 528), as calculated from 36 evaluable curves.

*Abnormal Parathyroids.* Time-activity curves from parathyroid regions generally resembled those of the thyroid (Fig. 1B). Results from 59 parathyroids and the thyroid glands of the same patients are summarized in Table 4. The mean $T_{1/2}$ value of hyperplastic parathyroids was practically equal to that of the thyroid. Parathyroid adenomas yielded a higher mean value than the corresponding thyroid glands, with a few adenomas showing extreme differences. Nevertheless, statistical significance was not established in this series. When adenomas were compared to hyperplasia with respect to tetrofosmin half-clearance times, statistical significance was reached (Student's t test: p = 0.002, Mann Whitney U test: p = 0.005).

In Figure 5, serial $^{99m}$Tc-tetrofosmin images from four studies are depicted. In the study shown in the first row, considerable retention of the tracer is observed in an adenoma

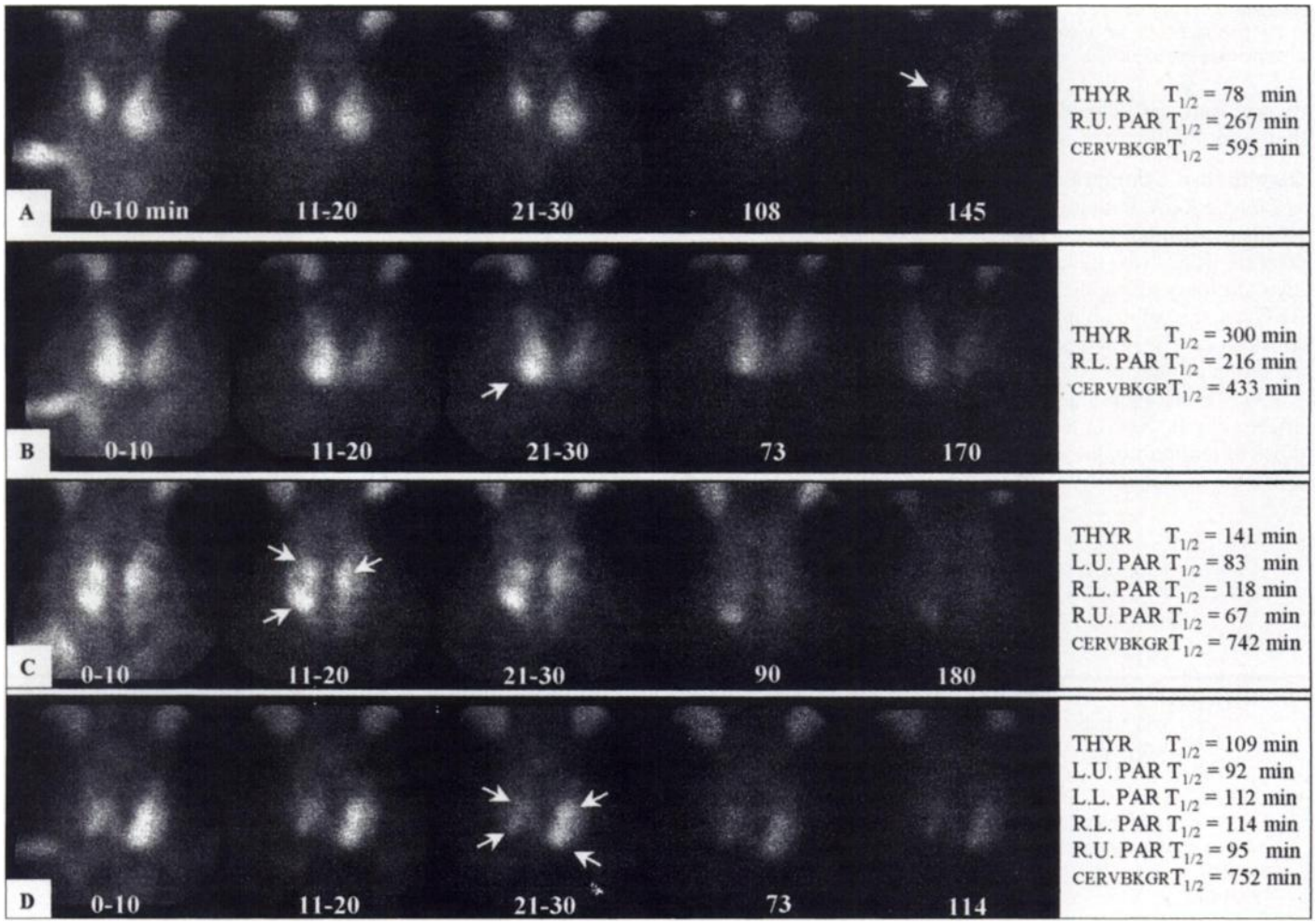


**FIGURE 5.** Selected serial tetrofosmin images in cases with solitary parathyroid adenomas (A and B) and hyperplasia (C and D). True positive findings are pointed by arrows. The calculated $T_{1/2}$ values from the thyroid (THYR), the abnormal parathyroids (PAR) and the cervical background (CERVBKGR) are listed on the right. The origin of the detected parathyroids (right or left, upper or lower) is abbreviated by initials. Variable tetrofosmin washout patterns in thyroid and parathyroid tissues are demonstrated.

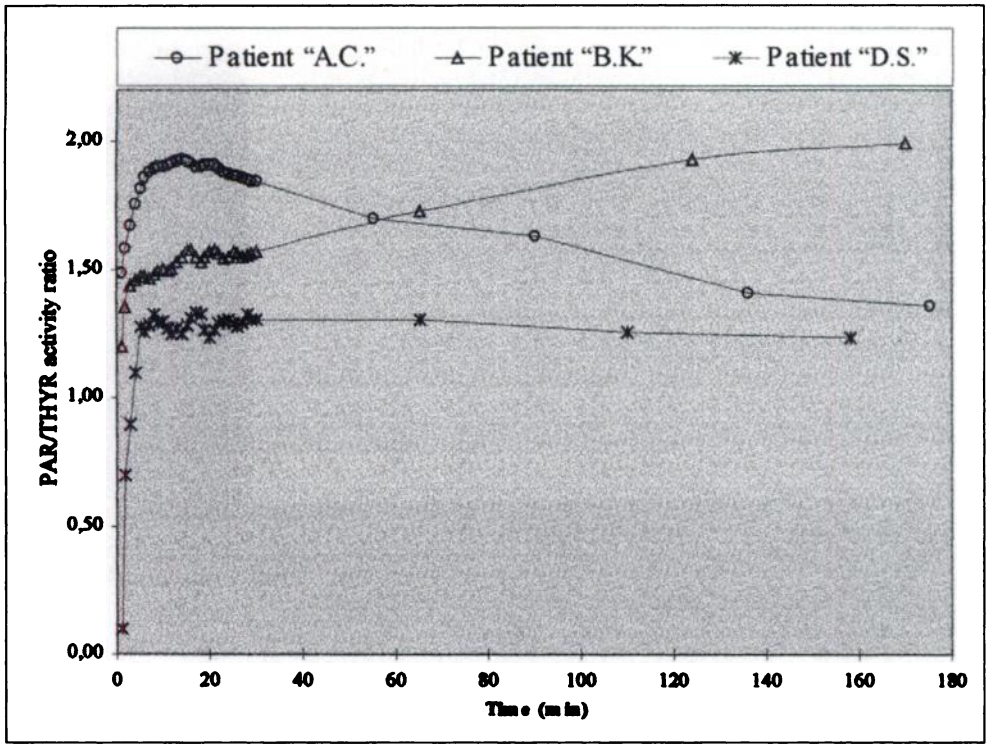


**FIGURE 6.** Curves representative of the observed patterns of parathyroid to thyroid count ratios plotted against time. Data are from three different patients: two with parathyroid adenoma (A.C. and B.K.) and one with parathyroid hyperplasia (D.S.). The most frequently observed pattern was that of patient A.C., showing a peak between 10 and 30 min.

of the right upper parathyroid compared to the parenchyma of the right thyroid lobe. In the same patient there is a large autonomous adenoma of the left thyroidal lobe, which also demonstrates some retention ($T_{1/2}$ = 120 min). In the second row, a right lower parathyroid adenoma shows faster clearance than the thyroid. The hyperplastic glands depicted in the lower two rows exhibit $T_{1/2}$ values either lower or only slightly higher than those of the corresponding thyroids; compared to the previously mentioned adenomas these half-times are all notably shorter.

*Factors Potentially Affecting Kinetic Results.* We used Spearman's test for correlation to determine whether the calculations of tetrofosmin clearance could have been affected by parathyroid gland size or count density and Mann-Whitney U test to assess the impact of lesion location (whether visualized inside or outside the thyroid borders) on kinetic results. We also tested a possible relation to the preoperative PTH levels in the group of parathyroid adenomas (this could not be accomplished in cases of multiple gland hyperfunction). No correlation between $T_{1/2}$ values and any of these factors could be established. Histologic examination of adenomatous or hyperplastic parathyroid glands with long half-clearance times did not show differences in cellular composition (percentage of oxyphil cells) from the rest. Moreover, there were no distinct histologic features to differentiate adenomas from hyperplasia.

*THYR/BKGR, PAR/BKGR and PAR/THYR.* Simple target-to-background ratios of uncorrected counts offer a different aspect of tracer kinetics, which is closer to the visual impression of how relative concentrations vary with time. The mean time to peak of the THYR/BKGR ratios (n = 57) and the PAR/BKGR ratios (n = 22) were 9.7 ± 6.3 and 17.9 ± 7.5 min, respectively. After this relatively early peak, all curves demonstrated a gradual decline. Plots of PAR/THYR ratios against time (n = 68) had a more variable appearance, which could be grossly represented by three patterns (Fig. 6). An apparently ascending pattern was observed in only four cases; it was found to correspond to marked differences in calculated half-clearance times between the parathyroid and the thyroid. The time that the PAR/THYR ratio peaked was not recorded on many occasions, because several curves did not exhibit a clear peak, and furthermore, sampling beyond the 30th min of the study included only three or four points at various time intervals. Considering only curves with a recognizable peak between 1 and 30 min (n = 40), the mean time to peak of the PAR/THYR ratio was 14.7 ± 4.9 min.

## DISCUSSION

In keeping with previously published works (*22–24*), our results indicate that parathyroid abnormalities can be successfully imaged with $^{99m}$Tc-tetrofosmin. Regarding the tetrofosmin-pertechnetate subtraction technique, the figures of sensitivity, specificity and accuracy found in this series (Tables 1 and 2) are comparable to those of other current imaging methods in a similar patient population (*12–17*). The implementation of a single-day protocol in the majority of our patients, by injecting pertechnetate 3 hr after tetrofosmin, did not seem to affect the quality of the thyroid scan, at least at the doses used. The contribution of the residual tetrofosmin activity to the subsequent thyroid scan was always found to be less than 10% in the thyroid region and less than 20% in the cervical background area. This technique exhibited a higher sensitivity than the conventional thallium–technetium scan, particularly in cases of parathyroid hyperplasia. There was only one hyperplastic parathyroid that escaped detection by TF/TC although visualized with thallium, albeit not without some skepticism about the abnormality being depicted in this case. The tetrofosmin images were visually superior to those of thallium despite background activity in the lateral neck and around the midline being slightly higher. Although the uptake patterns of the two tracers appeared similar on occasions of thyroid nodularity, the false-positive rate of the TF/TC subtraction technique was lower (Table 2). This could be explained either by a lower uptake ratio of nonfunctioning nodules to normal thyroid with tetrofosmin compared to thallium, inversely by a higher uptake of the former agent by abnormal parathyroids relative to that by the thyroid or by both possibilities (Figs. 2 and 4). In all patients with autonomously functioning thyroid adenomas, despite the

presence of prominent subtraction artifacts induced by oversubtraction of the thyroid adenomas and undersubtraction of the suppressed thyroid parenchyma, correct diagnosis was possible with tetrofosmin due to the avid uptake of this agent in the parathyroid tumor in excess of that in all types of thyroid tissue; this was not true with thallium (Fig. 3).

Quantitative comparison of thallium and tetrofosmin demonstrated significant differences between the two tracers with respect to their relative concentrations in the abnormal parathyroids, the thyroid and the cervical background area. The parathyroid to thyroid and the parathyroid to background activity ratios were higher with tetrofosmin than with thallium, whereas in the group of patients with normal renal function the thyroid to background ratios were lower (Table 3). This apparently reflects differences in uptake mechanisms of the two agents as well as in the cellular composition and the blood supply of parathyroid and thyroid tissues. The cellular uptake of thallium has been shown to be higher than that of $^{99m}$Tc-tetrofosmin (*25*). The entrance of thallium into the cell is energy dependent, related to cell membrane potential and $K^+$,$Na^+$-ATPase activity (*26,27*). Tetrofosmin uptake mechanisms have not yet been extensively investigated; entrance in the cell is probably accomplished by passive diffusion as for other lipophilic compounds (*28*), although partial dependence on the cell $K^+$,$Na^+$ pump has been indicated by a recent study (*25*). Inside the cell, retention of tetrofosmin is determined by transmembrane electric potentials, which are related to the mitochondriac content and the functional status of the cell (*25*). Different mechanisms predominate in different cell models (*25,29*). Impaired trapping of tracers by the thyroid of patients with severe renal insufficiency impacts on the quality of images and is one of the reasons for the lower sensitivity of parathyroid scintigraphy in this clinical setting (*6,10,29*). In our series, a significant difference in the THYR/BKGR ratio of thallium was shown ($p = 0.013$, Mann-Whitney U test) between patients with primary hyperparathyroidism (normal renal function) and those with secondary hyperplasia (end-stage renal disease), contrary to $^{99m}$Tc-tetrofosmin for which no such difference could be detected ($p = 0.28$). The fact that the quality of the tetrofosmin scan seems less affected by renal failure presents an advantage over thallium in cases of secondary hyperplasia. Better count statistics, due to the higher dose administered, and superior imaging characteristics of $^{99m}$Tc may also favor the use of tetrofosmin.

Our kinetic results for $^{99m}$Tc-tetrofosmin indicate that, unlike $^{99m}$Tc-sestamibi (*16,17*), most parathyroid glands do not show significant retention of this tracer relative to the thyroid. On visual interpretation, only 3 of 20 adenomas and 1 of 49 hyperplastic glands were undoubtedly visualized better in the delayed views than in the early ones. Single-tracer washout interpretations without the aid of subtraction suffered from a loss of both sensitivity and specificity (Table 2). Quantification yielded similar results (Table 4). More than half of the hyperplastic glands and 7 of 17 adenomas demonstrated faster clearance than the thyroid, while only a small minority exhibited relative retention with a noticeable difference in the corresponding half-clearance times. Our results are in concordance with those of Giordano et al. (*23*), who in comparing $^{99m}$Tc-tetrofosmin and $^{99m}$Tc-sestamibi for parathyroid imaging, reported that the dual-phase accuracy was 59% for the former and 88% for the latter agent. In other studies, however, parathyroid half-retention times of tetrofosmin did not differ significantly from those of sestamibi (*22*). Uptake and washout patterns of both agents in tumor cell lines have not shown substantial differences (*26*). Both agents have been shown to be substrates of P-glycoprotein, a known transmembrane pump that acts as a natural cellular defense mechanism for the efflux of xenobiotics (*30,31*). Recent studies by Arbab et al. (*25*) have provided evidence that, unlike sestamibi, which resides mainly inside the mitochondria (*28,32*), the major fraction of tetrofosmin is in the cytosol; nevertheless, the cellular mitochondria content affects tetrofosmin uptake. One could speculate that the different responses of the two agents to the cellular and mitochondrial membrane electric potential gradients in the parathyroids cells, the thyroid, or both tissue types probably account for their dissimilar differential washout patterns, as implied by our results.

When tetrofosmin washout from adenomas was compared to that from hyperplastic glands, a significant difference was shown between the two groups. It does not appear probable that this difference is related to the size, intensity of uptake, functional status or histology of parathyroid tumors, since tetrofosmin clearance was not found to correlate with any of these factors. Consequently, we cannot find a reasonable explanation for this observed diversion in tetrofosmin washout patterns. The differential diagnosis between adenoma and hyperplasia cannot be accomplished preoperatively by any diagnostic means, and it is difficult and often impossible even for the pathologist (*33*). If diagnosis could be aided by kinetic studies of a radioactive agent it would be of interest, especially in cases of primary hyperparathyroidism. In our series, however, the primary hyperplastic parathyroid glands were a minority in the group with hyperplasia. It is not certain whether kinetics in secondary hyperplasia can be extrapolated to primary hyperplasia as well. Furthermore, the overlap of values between the two groups makes the practical diagnostic value of this difference questionable.

## CONCLUSION

Technetium-99m-tetrofosmin is a suitable tracer for parathyroid scintigraphy. The reconstitution kit is easily handled and does not require boiling. The kinetics of $^{99m}$Tc-tetrofosmin in thyroid and parathyroid tissues does not seem to warrant single-tracer washout studies, although delayed views can be helpful in a limited number of cases. Consequently, subtraction has to be applied to discriminate enlarged parathyroids from the adjacent thyroid, unless perhaps SPECT is used. Acquisition times between 10 and 30 min postinjection are probably most appropriate, ensuring clear thyroid delineation, adequate count statistics, sufficiently low background activity and peak parathyroid-to-thyroid activity ratio in most cases. Hyperplastic parathyroids probably demonstrate a faster washout than parathyroid adenomas, but further studies are needed to substantiate this observation and to determine its clinical impact. Tetrofosmin subtraction seems superior to thallium subtraction in respect to sensitivity, particularly in the setting of parathyroid hyperplasia, and also to specificity. For purposes of patient and laboratory convenience a single day protocol is possible by performing the thyroid scan with $^{99m}$Tc-pertechnetate a few hours after $^{99m}$Tc-tetrofosmin administration. In concordance with previous works, the current study reports satisfactory performance of $^{99m}$Tc-tetrofosmin parathyroid scintigraphy and thus indicates that it may be considered as an addition to the existing localization methods for the preoperative investigation of hyperparathyroidism.

## REFERENCES

1. Ferlin G, Borsato N, Camerani M, Conte N, Zotti D. New perspectives in localizing enlarged parathyroids by technetium-thallium subtraction scan. *J Nucl Med* 1983;24: 438–411.

2. Winzelberg GG, Hydovitz JD. Radionuclide imaging of parathyroid tumors: historical perspectives and new techniques. *Semin Nucl Med* 1985;15:161–170.
3. Hauty M, Swartz K, McClung M, Lowe DK. Technetium thallium subtraction scintiscanning for localization of parathyroid adenomas and hyperplasia: a reappraisal. *Am J Surg* 1987;153:479–486.
4. Miller DL, Doppman JL, Shawker TH, et al. Localization of parathyroid adenomas in patients who have undergone surgery. I. Noninvasive imaging methods. *Radiology* 1987;162:133–137.
5. Sandrock D, Merino MJ, Norton JA, Neuman RD. Parathyroid imaging by Tc/Tl scintigraphy. *Eur J Nucl Med* 1990;16:607–613.
6. Coackley AJ. Parathyroid localization: how and when [Editorial]? *Eur J Nucl Med* 1991;18:151–152.
7. Beierwaltes WH. Endocrine images: parathyroid, adrenal cortex and medulla and other endocrine tumors. Part 2. *J Nucl Med* 1991;32:1627–1639.
8. Takagi H, Tominaga Y, Ushida K, et al. Comparison of imaging methods for diagnosing enlarged parathyroid glands in chronic renal failure. *J Comput Assist Tomogr* 1985;9:733–737.
9. Moolenaar W, Heslinga JM, Arndt JW, van der Velde CG, Pauwels EK, Valentijn RM. Thallium-201/$^{99m}$Tc subtraction scintigraphy in secondary hyperparathyroidism in chronic renal failure. *Nephrol Dial Transplant* 1988;2:166–168.
10. Adalet I, Hawkins T, Clark F, Wilkinson R. Thallium-technetium scintigraphy in secondary hyperparathyroidism. *Eur J Nucl Med* 1994;21:509–513.
11. Coackley J, Kettle AG, Wells CP, O'Doherty MG, Collins REC. Technetium-99m sestamibi: a new agent for parathyroid imaging. *Nucl Med Commun* 1989;10:791–794.
12. O'Doherty MJ, Kettle AG, Wells CP, Collins REC, Coakley AJ. Parathyroid imaging with technetium-99m-sestamibi: preoperative localization and tissue uptake studies. *J Nucl Med* 1992;33:313–318.
13. Geatti O, Shapiro B, Orsulom P, et al. Localization of parathyroid enlargement: experience with technetium-99m methoxyisobutyl isonitrile and thallium-201 scintigraphy, ultrasound and CT. *Eur J Nucl Med* 1994;21:17–22.
14. Chen CC, Skarulis MC, Fraker DL, Alexander R, Marx SJ, Spiegel AM. Technetium-99m sestamibi imaging before reoperation for primary hyperparathyroidism. *J Nucl Med* 1995;36:2186–2191.
15. McBiles M, Lambert AT, Cote MG, Kim SY. Sestamibi parathyroid imaging. *Semin Nucl Med* 1995;25:221–234.
16. Taillefer R, Boucher Y, Potvin C, Lambert R. Detection and localization of parathyroid adenomas in patients with hyperparathyroidism using a single radionuclide imaging procedure with technetium-99m-sestamibi (double phase study). *J Nucl Med* 1992;33:1801–1807.
17. Billotey C, Aurengo A, Najean Y, et al. Identifying abnormal parathyroid glands in the thyroid uptake area using technetium-99m-sestamibi and factor analysis of dynamic structures. *J Nucl Med* 1994;35:1631–1636.
18. Kelly JD, Foster AM, Higley B, et al. Technetium-99m-tetrofosmin as a new radiopharmaceutical for myocardial perfusion imaging. *J Nucl Med* 1993;34:222–227.
19. Wackers FJT, Berman DS, Maddahi J, et al. Technetium-99m hexakis 2-methoxy-isobutyl isonitrile: human biodistribution, dosimetry, safety, and preliminary comparison to thallium-201 for myocardial perfusion imaging. *J Nucl Med* 1989;30:301–311.
20. Higley B, Smith FW, Smith T, et al. Technetium-99m-1,2-bis[bis(2-ethoxyethyl) phosphino]ethane: human biodistribution, dosimetry and safety of a new myocardial perfusion imaging agent. *J Nucl Med* 1993;34:30–38.
21. Ishibashi M, Nishida H, Kumabe T, et al. Tc-99m tetrofosmin. A new diagnostic tracer for parathyroid imaging. *Clin Nucl Med* 1995;20:902–905.
22. Aigner RM, Fueger GF, Nicoletti R. Parathyroid scintigraphy: comparison of technetium-99m methoxyisobutylisonitrile and technetium-99m tetrofosmin studies. *Eur J Nucl Med* 1996;23:693–696.
23. Giordano A, Meduri G, Marrozi P, et al. Technetium-99m-tetrofosmin in parathyroid scintigraphy [Abstract]. *Eur J Nucl Med* 1996;23:1057.
24. Huglo D, Beauchat V, Prangere T, et al. Technetium-99m-tetrofosmin for parathyroid imaging [Abstract]. *Eur J Nucl Med* 1996;23:1057.
25. Arbab AS, Koizumi K, Toyama K, Araki T. Uptake of technetium-99m-tetrofosmin, technetium-99m-MIBI and thallium-201 in tumor cell lines. *J Nucl Med* 1996;37:1551–1556.
26. De Jong M, Bernard BF, Breeman WAP, et al. Comparison of uptake of $^{99m}$Tc-MIBI, $^{99m}$Tc-tetrofosmin and $^{99m}$Tc-Q12 into human breast cancer cell lines. *Eur J Nucl Med* 1996;23:1361–1366.
27. McCall D, Zimmer LJ, Katz AM. Kinetics of thallium exchange in culture rat myocardial cells. *Circ Res* 1985;56:370–376.
28. Piwnica-Worms D, Kronauge JF, Chiu ML. Uptake and retention of hexakis (2-methoxy-isobutyl isonitrile) technetium(I) in cultured chick myocardial cells. *Circulation* 1990;82:1826–1838.
29. Brismar T, Collin VP, Kesselberg M. Thallium-201 uptake relates to membrane potential and potassium permeability in human glioma cells. *Brain Res* 1989;50:30–36.
30. Piwnica-Worms D, Chiu ML, Budding M, et al. Functional imaging of multidrug-resistant P-glycoprotein with an organo-technetium complex. *Cancer Res* 1993;53:997–984.
31. Ballinger JR, Bannerman J, Boxen I, Firby P, Hartman NG, Moore MJ. Technetium-99m-tetrofosmin as a substrate for P-glycoprotein: in vitro studies in multidrug-resistant breast tumor cells. *J Nucl Med* 1996;37:1578–1582.
32. Carvalho PA, Chiu ML, Kronauge JF, et al. Subcellular distribution and analysis of technetium-99m-MIBI in isolated perfused rat hearts. *J Nucl Med* 1992;33:1516–1522.
33. Arnaud CD, Kolb FO. The calciotropic hormones and metabolic bone disease. Disorders of parathyroid function. In: Greenspan FS, ed. *Basic and clinical endocrinology*, 3rd ed. Norwalk, CT: Appleton and Lange; 1991:263–290.

# Preoperative Localization of Parathyroid Lesions in Hyperparathyroidism: Relationship Between Technetium-99m-MIBI Uptake and Oxyphil Cell Content

André Carpentier, Simon Jeannotte, Jean Verreault, Bernard Lefebvre, Guy Bisson, Charles-Jacques Mongeau and Pierre Maheux

*Department of Medicine, Division of Endocrinology and Metabolism and Departments of Nuclear Medicine and Pathology, Faculté de Médecine, Université de Sherbrooke, Québec, Canada*

The aim of this study was to assess the relationship between parathyroid oxyphil cell content and early or late phases of uptake of $^{99m}$Tc-MIBI, a radioisotope preferentially retained in mitochondria-rich cells. **Methods:** This study is a retrospective, single-blind analysis of all double-phase $^{99m}$Tc-MIBI parathyroid scintigraphy studies performed before surgery in our institution between 1990 and 1995. A total of 18 parathyroid lesions in 14 patients were reviewed. This sample included 11 cases of primary hyperparathyroidism (8 adenomas, 1 adenocarcinoma and 2 hyperplasias) and 3 cases of tertiary hyperparathyroidism secondary to chronic renal failure. **Results:** Uptake of $^{99m}$Tc-MIBI in the early phase of scintigraphy was associated with larger parathyroid lesions (1.61 ± 1.61 ml versus 0.33 ± 0.27 ml; $p < 0.02$) and higher serum calcium levels (3.00 ± 0.41 m*M* versus 2.67 ± 0.14 m*M*; $p < 0.02$). More importantly, we found that a parathyroid oxyphil cell content greater than 25% was more often associated with a positive uptake of $^{99m}$Tc-MIBI in the late phase of the test (positive late uptake in 78% of lesions with a high oxyphil cell content versus 33% in lesions with an oxyphil cell content between 1% and 25% and 0% in lesions with no oxyphil cells; $p < 0.04$). **Conclusion:** These findings suggest that the late retention of $^{99m}$Tc-MIBI in double-phase scintigraphy is related to parathyroid oxyphil cell content.

**Key Words:** hyperparathyroidism; technetium-99m-MIBI; oxyphil cells; parathyroid adenoma

**J Nucl Med 1998; 39:1441–1444**

Technetium-99m-MIBI was introduced in 1989 as a novel radioisotope for parathyroid imaging. Subtraction imaging methods using this isotope in combination with $^{123}$I or $^{99m}$Tc-pertechnetate were initially shown to be superior to other scintigraphic or radiological techniques (*1–5*). These tech-

Received June 16, 1997; revision accepted Oct. 23, 1997.

For correspondence or reprints contact: Pierre Maheux, MD, Division of Endocrinology and Metabolism, Centre Universitaire de Santé de l'Estrie (Fleurimont), 3001, 12ème Avenue Nord, Sherbrooke, Québec, J1H 5N4, Canada.